Turkish Journal of Electrical Engineering and Computer Sciences

Volume 24 | Number 6 Article 31

1-1-2016

Minimum number of permanent-magnet synchronous generators for coordinated low-voltage ride-through of induction generators in hybrid wind farms

SHENGHU LI

RUI AN

Turkish Journal of Electrical Engineering & Computer Sciences

http://journals.tubitak.gov.tr/elektrik/

Research Article

Turk J Elec Eng & Comp Sci
(2016) 24: 4970 – 4983

doi:10.3906/elk-1411-96

Minimum number of permanent-magnet synchronous generators for coordinated low-voltage ride-through of induction generators in hybrid wind farms

Shenghu LI*, Rui AN
School of Electrical Engineering and Automation, Hefei University of Technology, Hefei, P.R. China

Received: 14.11.2014 • **Accepted/Published Online:** 12.10.2015 • **Final Version:** 06.12.2016

Abstract: Coordinated low-voltage ride-through (LVRT) of induction generators (IGs) utilizing the excessive reactive power of permanent magnet synchronous generators (PMSGs) in hybrid wind farms is attractive due to saving investments on shunt compensators. The existing research is mainly based on dynamic simulations to given scenarios and does not quantify the necessary capacity and number of PMSGs. This paper newly proposes an analytical model to quantify the minimum number of the PMSGs for coordinated LVRT. The critical voltage at the point of common coupling (PCC) leading to slip instability of the IGs is quantified. To avoid instability, necessary var support from the PMSGs to improve the PCC voltage above the critical value is proposed. With the improved var control to the grid-side converter (GSC), the minimum number of PMSGs is determined. Numerical results are provided to validate any error of the proposed model, which shows that voltage drop at the PCC, power capability of the PMSGs, and control strategy of the GSC are the critical factors for coordinated LVRT.

Key words: Low-voltage ride-through, coordinated low-voltage ride-through, induction generator, permanent magnet synchronous generator, critical voltage, grid code

1. Introduction

The increasing use of wind power has had a notable effect on power systems [1], and thus grid codes for wind turbine generators (WTGs), e.g., low-voltage ride-through (LVRT) requirements, are set by the International Electrotechnical Commission (IEC) [2] and different power utilities. When they suffer from voltage drops after grid faults, the WTGs are expected to keep integration, increase var output to maintain the voltage at the point of common coupling (PCC), and shorten the postfault recovery process.

Due to simple configuration and low cost, induction generators (IGs) were applied for wind energy conversion in the early stages and are still in service in many wind farms. They absorb reactive power, and, after a fault, the rotor may suffer from slip instability [3,4] or speed stability [5]. The shunt compensator helps to improve voltage profile and stability [6], but it needs additional investment. The series dynamic braking resistor is also a possible choice [7], but it adds resistive loss during LVRT. Permanent-magnet synchronous generators (PMSGs) use back-to-back converters and spare the gearbox compared with IGs and doubly fed induction generators (DFIGs) [8,9]. LVRT may also be realized by improving the control strategy [10] or using energy storage systems and braking choppers [11]. The former has a limited response speed to active power, and the latter needs investment.

*Correspondence: shenghuli@hfut.edu.cn

This paper does not intend to contradict the existing LVRT methods; a parallel resistor with a DC link is used for PMSGs. The focus is on coordinated LVRT to the IGs using the excessive reactive power of the PMSGs. The var capability of variable-speed WTGs is given by a grid-side converter (GSC) and is wider than IGs [12], especially under dispatch mode [13]. If the PMSGs are installed after the IGs to form a hybrid wind farm, the excessive reactive power of the former may be utilized to improve the voltage profile at PCC and help the LVRT of the IGs.

It should be noted that the main task of newly installed PMSGs is wind energy conversion. However, if PMSGs are to be installed, careful design and control helps the LVRT of IGs and thus spares the need for investment in shunt compensators, which is about 45–55 $/kvar [14]. With coordinated LVRT, the only investment is the possible increment of the GSC of the PMSGs. With the help of PMSGs, IGs can provide active outputs during faults, which yields a production increment due to coordinated LVRT. However, the yearly production is difficult to compare, since fault occurrence is probabilistic, and the effect of grid integration of the IGs is associated with system performance.

Coordinated LVRT between fixed- and variable-speed WTGs has become attractive in recent years. Teninge et al. studied the ride-through of the IG with the help of PMSGs [15], where the GSC of the latter served as a static synchronous compensator (STATCOM) to provide var support. Muyeen and Sarkhanloo studied LVRT of the IG with the help of PMSGs and DFIGs, respectively [16,17]. The former used feedback decomposition, while the latter applied direct power control. Rosyadi et al. applied fuzzy logic to PMSGs for coordinated LVRT [18]. The work was extended in [19] to quantify the ratio of the WTGs for coordinated LVRT. These pioneering works were based on dynamic simulations to given numbers of WTGs, which is accurate but time-consuming. Furthermore, it is difficult to decide the minimum number of PMSGs to guarantee coordinated LVRT and the critical factors/parameters.

Therefore, an analytical solution for coordinated LVRT, instead of repeated tests, will be more convenient for practical applications and it helps to find critical factors to decide the units of PMSGs following the grid code. The difficulty in finding the minimum number of PMSGs is the critical voltage of the PCC, i.e. the lowest voltage at the PCC that ensures grid integration of the WTGs, whose solution is similar to the critical clearing time (CCT) of IGs. Grilo et al. proposed an analytical method to find the CCT when the grid voltage drops to 0 [20], but voltage drop prescribed in different grid codes is not necessarily 0.

This paper studies the coordinated LVRT for hybrid wind farms with both PMSGs and IGs. An analytical model to quantify the minimum number of PMSGs is newly proposed. First the critical PCC voltage leading to instability of the IGs is quantified, and the possible voltage drop at the PCC following the grid code is quantified. Then the slip stability of the IGs is judged by comparing the critical voltage with the severest voltage drop. The necessary var support from the PMSGs to avoid instability is quantified. Finally, with improved var control to the GSC, the minimum number of PMSGs is determined. The numerical results are provided to validate the error of the proposed method and analyze the influencing factors of the coordinated LVRT scheme.

2. Critical PCC voltage for slip stability of IGs

As shown in Figure 1, the PMSG and IG in the hybrid wind farm are stepped up to the PCC through transformers T_A and T_B, while the PCC is stepped up to the equivalent system bus through transformer T_C and line L. V_{PCC} and V_{sys} are the voltages of the PCC and the system; X_{TA}, X_{TB}, and X_{TC} are the reactances of transformers T_A, T_B, and T_C; R_g and X_g are the resistance and reactance of the GSC; R_L and X_L are the resistance and reactance of the transmission line; R_{CB} is the crowbar of the DC link; and S_{PMSG}, S_{IG}, and S_{PCC} are the apparent power of the PMSG, IG, and PCC.

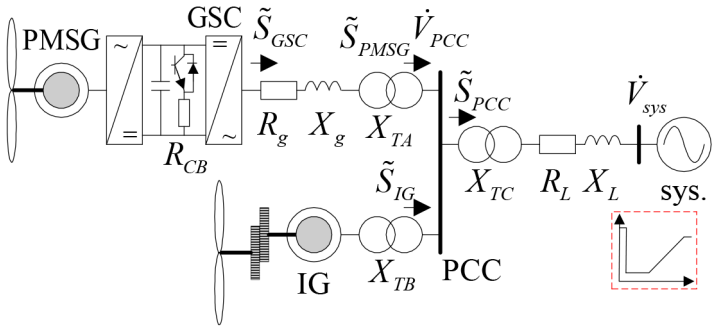

Figure 1. Configuration of hybrid wind farm.

The equivalent circuit of the IG and T $_B$ is shown in Figure 2a, which is simplified in Figure 2b using Thevenin's theorem. The equivalent voltage and equivalent impedance are given by:

$$\dot{V}_{TH} = \frac{jX_m}{R_s + j(X_s + X_{TB}) + jX_m}\dot{V}_{PCC}, \tag{1}$$

$$Z_{TH} = \frac{[R_s + j\,(X_s + X_{TB})]\,jX_m}{R_s + j\,(X_s + X_{TB}) + jX_m} = R_{TH} + jX_{TH}, \tag{2}$$

where R_s, X_s, R_r, and X_r are the resistance and reactance of the stator and rotor; X_m is the magnetizing reactance; s is the slip; V_{TH} is the equivalent voltage; R_{TH} and X_{TH} are the equivalent resistance and reactance; and Z_{TH} is the equivalent impedance.

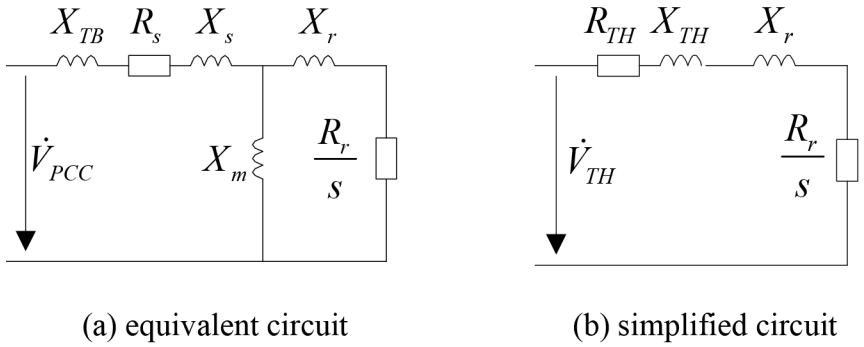

Figure 2. Equivalent circuit of IG: (a) equivalent circuit, (b) simplified circuit.

The electromagnetic torque T_E is defined by Eq. (3) and is obviously dependent on s and V_{TH}.

$$T_E = \frac{sR_rV_{TH}^2}{(sR_{TH} + R_r)^2 + s^2(X_{TH} + X_r)^2} \tag{3}$$

Since s of the IG is usually quite small, sR_{TH} is much less than R_r and is thus ignored. T_E is simplified to:

$$T_E = \frac{sR_rV_{TH}^2}{R_r^2 + s^2(X_{TH} + X_r)^2}. \tag{4}$$

The mechanical torque of the wind turbine (WT) T_M is given by:

$$T_M = \frac{C_P\rho\pi R^2v^3}{2(1-s)\omega_sS_N}, \tag{5}$$

where C_P is the power coefficient of the WT, ρ is the air density, R is the radius of wind turbine, v is the wind speed, ω_s is the synchronous speed, and S_N is the base capacity.

With the single-mass model for the drive train, the motion equation is given by:

$$2\left(H_T + H_G\right)\frac{ds}{dt} = -T_M - T_E, \tag{6}$$

where H_T and H_G are the inertia constants of the wind turbine and generator. By substituting T_E and T_M, Eq. (6) is rewritten as:

$$k_5\frac{ds}{dt} = -k_1 + \frac{sk_2}{k_3 + s^2k_4}, \tag{7}$$

where $k_1 = T_M$, $k_2 = -V_{TH}^2R_r$, $k_3 = R_r^2$, $k_4 = (X_{TH} + X_r)^2$, and $k_5 = 2(H_T + H_G)$. It is clear that k_3, k_4, and k_5 are constants. Since the fault duration prescribed by the grid code is very short, the active power captured by the WT is almost constant, so with limited change of the rotor slip, k_1 may also be seen as a constant.

During the normal operation, the left side of Eq. (7) is zero, and thus the initial slip s_0 and the critical slip s_{cr} are given by:

$$\begin{cases} s_0 = \frac{k_2+\sqrt{\beta}}{2k_1k_4} \\ s_{cr} = \frac{k_2-\sqrt{\beta}}{2k_1k_4} \end{cases}, \tag{8}$$

where $\beta = k_2^2 - 4k_1^2k_3k_4 > 0$. By setting $\beta = 0$, the maximum critical voltage is given by:

$$V_{TH,cr\max} = \sqrt{\frac{\sqrt{4k_1^2k_3k_4}}{R_r}}. \tag{9}$$

Eq. (9) is explained as follows. With a grid fault, k_2 changes to $k_2^{'}$, where $k_2^{'} = -V_{TH}^{'2}R_r$, and the voltage drop at the PCC changes the electromagnetic torque and the torque balance. With a minor voltage drop, $V_{TH}^{'}$ is larger than $V_{TH,cr\max}$. There are 2 solutions as shown in Eq. (8), i.e. 2 intersections of the mechanical and electromagnetic torques, corresponding to $\beta > 0$. Since the mechanical torque is larger than the electromagnetic torque, the rotor starts to accelerate. Then the torque is balanced, and the rotor speed is fixed; the IG stays stable during the fault. With more voltage drop, $V_{TH}^{'}$ is equal to $V_{TH,cr\max}$, and the electromagnetic and the mechanical torques have only 1 intersection, corresponding to $\beta = 0$. The IG is critically stable. With a major voltage drop, $V_{TH}^{'}$ is lower than $V_{TH,cr\max}$, and the mechanical torque is larger than the electromagnetic torque during fault, i.e. there is no intersection, corresponding to $\beta < 0$, which may yield slip instability.

The slip stability is dependent on the integral to Eq. (7) within the fault duration. When $V_{TH}^{'}$ is smaller than $V_{TH,cr\max}$, the right side of Eq. (7) is no longer equal to 0 during a fault. Moving the terms including time and slip to different sides, Eq. (10) is yielded. Its right side has 3 parts. The 1st part is easy to solve.

$$dt = k_5\frac{k_4s^2 + k_3}{-k_1k_4s^2 + k_2^{'}s - k_1k_3}ds = -\frac{k_5}{k_1k_4}\left(k_4 + \frac{k_2^{'}}{2k_1}\frac{2s - \frac{k_2^{'}}{k_1k_4}}{s^2 - \frac{k_2^{'}}{k_1k_4}s + \frac{k_3}{k_4}} + \frac{k_2^{'}}{2k_1}\frac{k_2^{'}}{k_1k_4}\frac{1}{s^2 - \frac{k_2^{'}}{k_1k_4}s + \frac{k_3}{k_4}}\right)ds \tag{10}$$

The integral to the 2nd part is given by:

$$\int -\frac{k_5}{k_1k_4}\frac{k_2^{'}}{2k_1}\frac{2s-\frac{k_2^{'}}{k_1k_4}}{s^2-\frac{k_2^{'}}{k_1k_4}s+\frac{k_3}{k_4}}ds=-\frac{k_5}{k_1k_4}\frac{k_2^{'}}{2k_1}\ln\left|s^2-\frac{k_2^{'}}{k_1k_4}s+\frac{k_3}{k_4}\right|. \tag{11}$$

The 3rd part is rewritten by:

$$-\frac{k_5}{k_1k_4}\frac{k_2^{'}}{2k_1}\frac{k_2^{'}}{k_1k_4}\frac{1}{s^2-\frac{k_2^{'}}{k_1k_4}s+\frac{k_3}{k_4}}ds=-\frac{k_5}{k_1k_4}\frac{k_2^{'}}{2k_1}\frac{k_2^{'}}{k_1k_4}\frac{1}{\left(s-\frac{k_2^{'}}{2k_1k_4}\right)^2+\frac{k_3}{k_4}-\frac{k_2^{'2}}{4k_1^2k_4^2}}ds. \tag{12}$$

For instable cases with $\beta<0$, there are 2 complex roots for the denominator, i.e. $s=a\quad\pm\,\mathrm{j}b$, corresponding to the postfault initial and critical slips, where

$$\begin{cases} a=\frac{k_2^{'}}{2k_1k_4} \\ b=\frac{k_3}{k_4}-\frac{k_2^{'2}}{4k_1^2k_4^2} \end{cases}. \tag{13}$$

Then the 3rd part is rewritten to:

$$-\frac{k_5}{k_1k_4}\frac{k_2^{'}}{2k_1}\frac{k_2^{'}}{k_1k_4}\frac{1}{(s-a)^2+b}ds=-\frac{k_5}{k_1k_4}\frac{k_2^{'}}{2k_1}\frac{k_2^{'}}{k_1k_4}\frac{1}{b}\frac{1}{\left(\frac{s-a}{\sqrt{b}}\right)^2+1}ds. \tag{14}$$

Finally, the complete solution to Eq. (7) is given by:

$$t_{f\max}=-\frac{k_5}{k_1k_4}\left[k_4s+\frac{k_2^{'}}{2k_1}ln\left|s^2-\frac{k_2^{'}}{k_1k_4}s+\frac{k_3}{k_4}\right|+\frac{k_2^{'2}}{2k_1^2k_4}\frac{1}{\sqrt{b}}\arctan\left(\frac{s-a}{\sqrt{b}}\right)\right]\Bigg|_{s_0}^{s_{cr}}, \tag{15}$$

where $t_{f\max}$ is the fault duration. By solving Eq. (15), $k_2^{'}$ and $V_{TH}^{'}$ are derived, where $V_{TH}^{'}$ is compared with $V_{TH,cr}$, and $V_{PCC,cr}$ is found. The equivalent voltage reduces to $V_{TH}^{'}$ and is below $V_{TH,cr\max}$. The unbalanced torque drives the rotor to accelerate, and the slip reaches s_{cr} when the fault time is $t_{f\max}$. When V_{PCC} is below $V_{PCC,cr}$, the slip may be less than s_{cr} and the IG may not keep slip stability. Oscillations of the slip, stator voltage, and active and reactive powers may occur. Obviously $V_{PCC,cr}$ is related to the inertia, the critical slip, the mechanical torque, the electric parameters of the IG, and the severity and duration of voltage drop prescribed by the grid codes.

3. PCC voltage following the LVRT rule

The PCC voltage is related to the system bus, while the lowest voltage at the system bus is defined by the grid code. The active and reactive outputs at the PCC are determined by the outputs of the PMSG and the IG. Since the system bus voltage and PCC power are located at different buses, V_{PCC} may be derived using an iterative method. To save calculation effort, a direct solution is proposed here.

The PCC voltage is described by:

$$\dot{V}_{PCC}=V_{sys}+\dot{I}_{PCC}Z_{tr}, \tag{16}$$

where $Z_{tr} = R_{tr} + \mathrm{j}X_{tr} = R_L + \mathrm{j}(X_{TC} + X_L)$. The power output of the PCC is defined as:

$$\tilde{S}_{PCC} = \dot{V}_{PCC}\dot{I}^*_{PCC}. \tag{17}$$

Substituting Eq. (17) into (16), one may get:

$$V^2_{PCC} - V_{sys}\dot{V}^*_{PCC} - \tilde{S}^*_{PCC}Z_{tr} = 0. \tag{18}$$

The equation is rewritten with the real and imaginary parts separately expressed:

$$\begin{cases} V_{sys}V_{PCC}\cos\theta_{PCC} = V^2_{PCC} - R_{tr}P_{PCC} - X_{tr}Q_{PCC} \\ V_{sys}V_{PCC}\sin\theta_{PCC} = X_{tr}P_{PCC} - R_{tr}Q_{PCC} \end{cases}, \tag{19}$$

where θ_{PCC} is the voltage phase angle of the PCC, and by eliminating θ_{PCC}, a fourth order equation with V_{PCC} is derived:

$$V^2_{sys}V^2_{PCC} = \left(V^2_{PCC} - R_{tr}P_{PCC} - X_{tr}Q_{PCC}\right)^2 + \left(X_{tr}P_{PCC} - R_{tr}Q_{PCC}\right)^2. \tag{20}$$

If V_{PCC} is lower than the critical voltage $V_{PCC,cr}$, slip instability of the IG may occur. If V_{PCC} should be higher than $V_{PCC,cr}$, reactive output Q_{PCC} needs to be increased.

4. Var support capability of the PMSG

4.1. Power outputs of the GSC

If the PMSG in the same wind farm increases var output, V_{PCC} will be improved and thus slip instability of the IG may be avoided. Coordinated LVRT capability is decided by the number and var ratings of the PMSGs, and the critical voltage at the PCC.

Assume there are n_{IG} IGs and n_{PMSG} PMSGs. The IGs have the same parameters and wind speeds and the same is true for the PMSGs. The total power injected to PCC is given by:

$$\begin{cases} P_{PCC} = n_{PMSG}P_{PMSG} + n_{IG}P_{IG} \\ Q_{PCC} = n_{PMSG}Q_{PMSG} + n_{IG}Q_{IG} \end{cases}. \tag{21}$$

The slip is time-dependent after a fault occurs. For the analytical solution, it is estimated by the average value:

$$s_{av} = \frac{s_0 + s_{cr}}{2}. \tag{22}$$

Then the active power and reactive power of the IG, i.e. P_{IG} and Q_{IG}, are given by:

$$\begin{cases} P_{IG} = -\frac{V^2_{TH,cr}R_r s_{av}}{R^2_r + s^2_{av}(X_{TH}+X_r)^2} \\ Q_{IG} = -\frac{V^2_{TH,cr}(X_{TH}+X_r)s^2_{av}}{R^2_r + s^2_{av}(X_{TH}+X_r)^2} \end{cases}. \tag{23}$$

Assume the d-axis is orientated by PCC voltage. The enhanced var control scheme utilizing available capacity of the GSC is shown in Figure 3, where V_{dc} is the DC voltage, Q_g is the reactive power of PCC, and I_{gd} and I_{gq} are the current of the GSC d axis and q axis. The subscript *set* presents the reference value. The maximum current of the GSC is $I_{g,lim}$. The current component along the d-axis maintains the DC voltage, while that along the q-axis decides the reactive output.

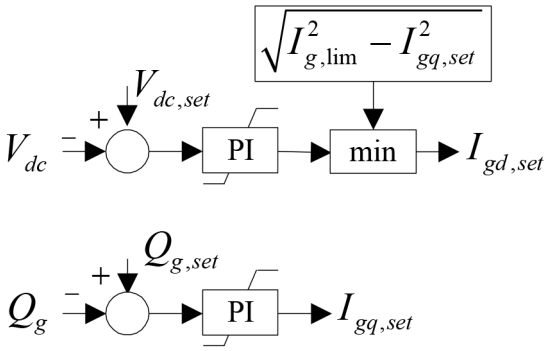

Figure 3. Enhanced var control for GSC.

To ensure the wind power generation and the maximum reactive power injected to the PCC, $Q_{g,set}$ is controlled to yield $I_{gq,set}$ close to the current limit of the GSC. The active power P_{PMSG} and reactive power Q_{PMSG} of PMSG are given by:

$$\begin{cases} P_{PMSG} = V_{PCC,cr}\sqrt{I_{g,\lim}^2 - I_{gq}^2} \\ Q_{PMSG} = -V_{PCC,cr} I_{gq} \end{cases} . \tag{24}$$

For the most serious consideration, the active and reactive outputs are approximately quantified by the powers injected to the PCC plus the maximum transmission loss, and the active power P_{GSC} and reactive power Q_{GSC} of the GSC are given by:

$$\begin{cases} P_{GSC} = P_{PMSG} + I_{g,\lim}^2 R_g \\ Q_{GSC} = Q_{PMSG} + I_{g,\lim}^2 (X_{TA} + X_g) \end{cases} . \tag{25}$$

4.2. Procedure of the proposed model

The coordinated LVRT scheme is summarized by following steps:

1) Calculate the critical PCC voltage leading to slip instability of the IG.

2) Set voltage at the system bus following the grid code, and calculate the lowest PCC voltage.

3) Compare the lowest PCC voltage with the critical value. If the former is lower than the latter, the PMSG is expected to increase var output.

4) Quantify var support capability of the PMSG and decide the minimum number of the PMSGs.

5) Compare the analytical results with those from the dynamic simulation to validate the error.

6) Analyze the contributing factors to the coordinated LVRT scheme.

7) It should be noted that the PMSGs have to guarantee LVRT themselves, implemented by the crowbar. Crowbar operation means less active output and thus more var support. Var support capability is related to the wind speed: higher speed corresponds to more active power output and thus less var capability. When the PMSG has rated active output, active power injection and unbalanced active power are the largest, forming the severest LVRT condition. Therefore, the coordinated LVRT with the PMSG at the rated power certainly satisfies other operation conditions.

To validate the LVRT effect, the equivalent system bus must suffer from the voltage drop prescribed by the grid code of China, e.g., voltage decreased to 0.2 p.u. and a duration of 0.625 s. The grid codes in different countries are different, but they share similar features, i.e. with prescribed voltage drops and durations. By changing these parameters, the proposed analytical LVRT scheme may be easily modified to adapt to other grid codes. For example, IEC 61400-21 requires an LVRT with voltage decreased to 0.2 p.u. and duration of 0.2 s. Thus, the analytical method may be applied by replacing the fault duration to 0.2 s, without changing the equations.

Compared with dynamic simulation, error exists with the analytical method due to an assumption of fixed mechanical torque during fault duration, the average slip, and the steady state instead of the transient model for the circuit windings. The study in [14] showed a CCT error of 10%–15% between the analytical result and simulation result for shunt compensation.

5. Minimum PMSGs from analytical model

The air density is ρ= 1.2041 kg/m^3. The radius of the WT is R= 27 m. The rated wind speed of the IG is 12.3 m/s. The PMSG and IG have rated power of 1 MW and rated voltage of 690 V. The base capacity is 1 MW. The base voltage is 690 V. There are 10 IGs in the hybrid wind farm, for which H_T = 2.5 s and H_G = 0.5 s. The stiffness and the damping coefficient are 0.3 p.u. and 1.5 p.u. respectively. R_s = 0.0121 p.u., X_s = 0.0742 p.u., R_r = 0.008 p.u., X_r = 0.1761 p.u., and X_m = 2.7626 p.u. For the PMSG, the permanent flux is 1.4 p.u. The inductances of the d and q axes are 1 p.u. and 0.7 p.u., respectively. R_g = 0.02 p.u., X_g = 0.02 p.u., R_{CB} = 6 p.u., $X_{TA} = X_{TB}$ = 0.08 p.u., Z_{tr} = 0.0005 + j0.005 p.u., and $I_{g,\lim}$ = 1.6 p.u.

At the rated power, the reactive current of the GSC is controlled to maintain the PCC voltage at 1.05 p.u. and the stator voltage of IG at 1.0 p.u. The related coefficients are given by:

$$k_1 = 1, \quad k_2 = -0.0078, \quad k_3 = 6.4 \times 10^{-5}, \quad k_4 = 0.1039.$$

By solving Eq. (8), β, s_0, and s_{cr} are given by:

$$\beta = 3.46 \times 10^{-5},$$

$$s_0 = \frac{-0.0078 + \sqrt{\beta}}{2 \times 0.1039} = -0.0093,$$

$$s_{cr} = \frac{-0.0078 - \sqrt{\beta}}{2 \times 0.1039} = -0.0660.$$

The postfault average slip s_{av} and the maximum critical voltage $V_{TH,cr\max}$ are given by:

$$s_{av} = \frac{s_0 + s_r}{2} = -0.03765,$$

$$V_{TH,crmax} = \sqrt{\frac{\sqrt{4 \times 1 \times 6.4 \times 10^{-5} \times 0.1039}}{0.008}} = 0.803.$$

Based on $V_{TH,cr\max}$, it is found that $V_{PCC,cr\max}$ equals 0.847 p.u.

The coefficients a and b are given by:

$$a = \frac{k_2^{'}}{2k_1k_4} = -0.0385V_{TH,cr}^2,$$

$$b = \frac{k_3}{k_4} - \frac{k_2'^2}{4k_1^2k_4^2} = 6.16 \times 10^{-4} - 0.0015V_{TH,cr}^4.$$

If we substitute s_0 and s_{cr} into Eq. (15), the start and the end of fault time, t_{st}, t_{en}, are given by:

$$\begin{aligned} t_{st} &= -57.7988 \times [0.1039s_0 - 0.004V_{TH,cr}^2 ln\left|s_0^2 + 0.0771V_{TH,cr}^2 s_0 + 6.2 \times 10^{-4}\right| \\ &+ \frac{3.1 \times 10^{-4} \times V_{TH,cr}^4}{\sqrt{6.16 \times 10^{-4} - 0.0015V_{TH,cr}^4}} a\tan\left(\frac{s_0 + 0.0385V_{TH,cr}^2}{\sqrt{6.16 \times 10^{-4} - 0.0015V_{TH,cr}^4}}\right)] \end{aligned}$$

$$\begin{aligned} t_{en} &= -57.7988 \times [0.1039s_{cr} - 0.004V_{TH,cr}^2 ln\left(\left|s_{cr}^2 + 0.0771V_{TH,cr}^2 s_{cr} + 6.2 \times 10^{-4}\right|\right) \\ &+ \frac{3.1 \times 10^{-4} \times V_{TH,cr}^4}{\sqrt{6.16 \times 10^{-4} - 0.0015V_{TH,cr}^4}} a\tan\left(\frac{s_{cr} + 0.0385V_{TH,cr}^2}{\sqrt{6.16 \times 10^{-4} - 0.0015V_{TH,cr}^4}}\right)]. \end{aligned}$$

By solving $t_{en} - t_{st} = 0.625$, $V_{TH,cr}$ is 0.5872 p.u., less than $V_{TH,crmax}$. The corresponding $V_{PCC,cr}$ is 0.62 p.u. The active and reactive powers by IGs injected to the PCC are given by:

$$\begin{cases} P_{IG} = -10 \times \frac{0.5872^2 \times 0.008 \times (-0.03765)}{0.008^2 + 0.03765^2 \times (0.1461 + 0.1761)^2} = 4.9184 \\ Q_{IG} = 10 \times \frac{0.5872^2 \times (0.1461 + 0.1761) \times (-0.03765)^2}{0.008^2 + 0.03765^2 \times (0.1461 + 0.1761)^2} = -7.4580 \end{cases}.$$

By controlling $I_{gq,set}$ at 1.55 p.u., active and reactive outputs by each PMSG are given by:

$$\begin{cases} P_{PMSG} = 0.62 \times \sqrt{1.6^2 - 1.55^2} = 0.246 \\ Q_{PMSG} = 0.62 \times 1.55 = 0.961 \end{cases}.$$

Then P_{GSC} and Q_{GSC} are given by:

$$\begin{cases} P_{GSC} = 0.246 + 1.6^2 \times 0.02 = 0.297 \\ Q_{GSC} = 0.961 + 1.6^2 \times (0.08 + 0.02) = 1.217 \end{cases}.$$

They satisfy the capacity restriction of the GSC:

$$\sqrt{P_{GSC}^2 + Q_{GSC}^2} = \sqrt{1.217^2 + 0.297^2} = 1.253 < S_{GSC,\lim} = 1.6.$$

The active and reactive powers of the hybrid wind farm injected into the PCC are given by:

$$\begin{cases} P_{PCC} = 4.9184 + 0.246n_{PMSG} \\ Q_{PCC} = 0.961n_{PMSG} - 7.4580 \end{cases}.$$

When the system voltage drops to 0.2 p.u., Eq. (20) is expressed as:

$$\begin{aligned} 0.2^2 \times 0.62^2 &= \left[0.62^2 - 0.0005\left(4.9184 + 0.246n_{PMSG}\right) - 0.005\left(0.961n_{PMSG} - 7.4580\right)\right]^2 \\ &+ \left[0.005\left(4.9184 + 0.246n_{PMSG}\right) + 0.0005\left(0.961n_{PMSG} - 7.4580\right)\right]^2. \end{aligned}$$

Reduce the above expression to:

$$2.689n_{PMSG}^2 - 420.44n_{PMSG} + 1.608 \times 10^4 = 0.$$

Solving the above equation, the minimum number of PMSGs n_{PMSG} is 67. However, as stated in Section 1, installation of the PMSGs is basically decided by the available wind sources; the second consideration is coordinated LVRT. If there are not sufficient wind sources, fewer PMSGs than expected for coordinated LVRT will be installed. Then shunt compensators are needed, which together with PMSGs guarantee LVRT of the IGs. With the larger capacity of GSCs, fewer PMSGs may be required for coordinated LVRT.

6. Minimum PMSGs from simulation results

In the following, the minimum number of PMSGs with the analytical method is validated by the dynamic simulation to quantify the error.

6.1. Critical voltage of IGs

If we set the PCC voltage at 0.90 p.u., 0.88 p.u., and 0.86 p.u., respectively, all higher than $V_{PCC,cr\max}$, then the rotor speed of the IGs is shown in Figure 4. It is found that higher PCC voltage yields lower stable rotor speed, consistent with the analytical model.

If we set the PCC voltage at 0.59 p.u. and 0.58 p.u., respectively, then the rotor speeds of the IGs are shown in Figure 5. The latter yields slip instability and thus the critical voltage is 0.59 p.u. The error of the analytical model is 0.03 p.u.

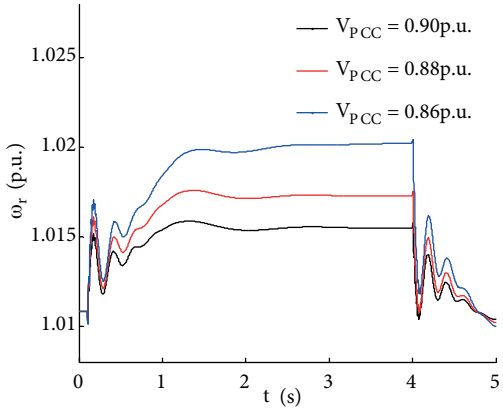

Figure 4. Voltage above maximum critical voltage at PCC keeping stability of IG.

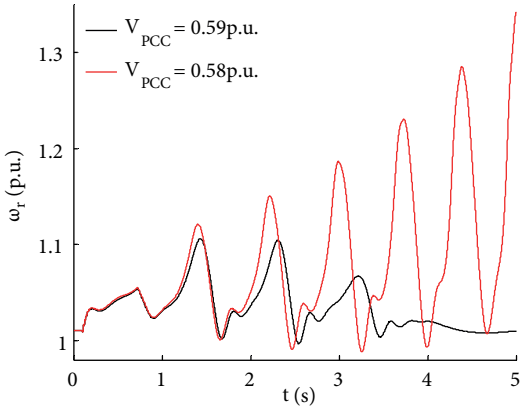

Figure 5. Critical voltage at PCC causing instability of IG.

The critical voltages are shown in Figures 6a–6f, with different calculation schemes, i.e. the inertia or rotor resistance of the IGs increased by 20%; the mechanical torque, stator reactance, or rotor reactance decreased by 20%; or the fault duration decreased by 20%.

It is found from Figures 6a–6d that increase of IG inertia or rotor resistance, or decrease of stator reactance or rotor reactance, yields an increase of the electromagnetic torque. The rotor accelerates more slowly and thus the critical voltage decreases to 0.54 p.u., 0.55 p.u., 0.54 p.u., and 0.43 p.u., respectively. With Figure 6e, shorter fault duration yields a shorter integration interval and less possibility to reach critical slip, and thus the

critical voltage decreases to 0.48 p.u. With Figure 6f, less mechanical torque yields a longer slip interval and smaller torque difference, and thus the critical voltage decreases to 0.22 p.u.

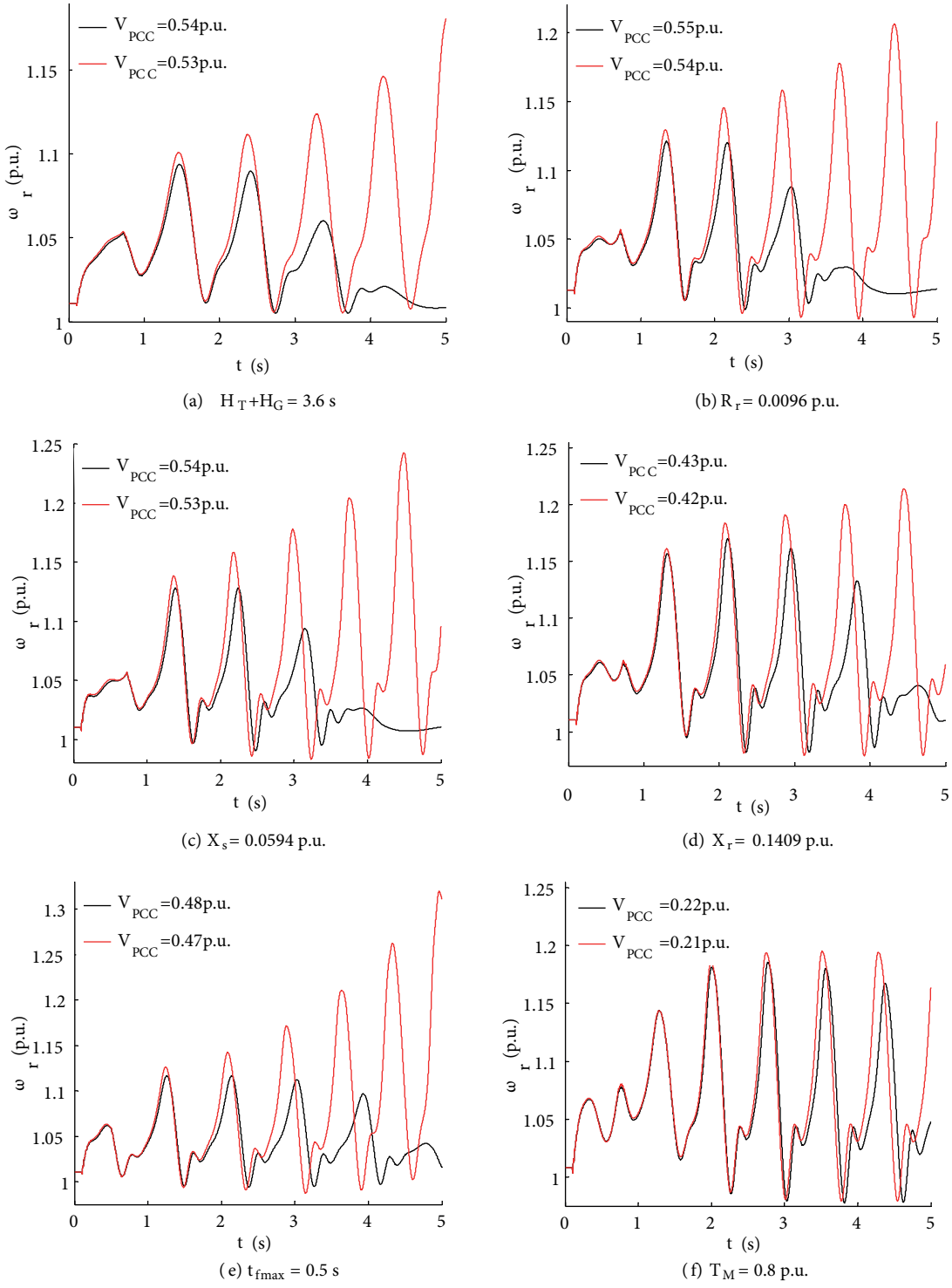

Figure 6. Contributing factors to critical voltage at PCC.

Therefore, larger inertia and rotor resistance, or less mechanical torque, stator reactance and rotor reactance, or shorter fault duration, yields a lower critical voltage. Comparing their impact on the critical voltage, the mechanical torque ranks the highest, followed by the rotor reactance, fault time, rotor resistance, inertia, and stator reactance.

6.2. Minimum number of PMSG for coordinated LVRT

The number of PMSGs is decreased from the minimum number (67) with the analytical model. When the number is 60, the IGs lose slip stability, i.e. the actual minimum number of PMSGs is 61, with error of $(67 - 61)/61 = 9.84\%$, which is acceptable compared with [14]. The results from the analytical model are more preservative and beneficial for LVRT.

The DC voltage and active and reactive powers of each PMSG injected to the PCC are shown in the Table. When the grid fault occurs, crowbar operation avoids overvoltage of the DC capacitor, and the PMSGs are more reactive for LVRT by increasing reactive current reference while supplying active power during a fault.

Table. PMSG's response with coordinated LVRT.

	$n_{PMSG} = 67$			$n_{PMSG} = 61$			$n_{PMSG} = 60$		
t (s)	P_{PMSG} (p.u.)	Q_{PMSG} (p.u.)	V_{dc} (V)	P_{PMSG} (p.u.)	Q_{PMSG} (p.u.)	V_{dc} (V)	P_{PMSG} (p.u.)	Q_{PMSG} (p.u.)	V_{dc} (V)
0.1	0.975	0.366	1200	0.975	0.340	1200	0.975	0.336	1200
0.11	0.338	0.557	1359	0.334	0.510	1363	0.333	0.502	1364
0.14	0.242	0.827	1365	0.238	0.784	1369	0.238	0.777	1370
0.4	0.251	0.978	1463	0.243	0.888	1468	0.243	0.873	1469
0.6	0.236	0.947	1421	0.241	0.869	1417	0.242	0.857	1416
0.8	0.968	0.652	1131	0.969	0.645	1130	0.970	0.643	1130
1.5	0.970	0.650	1155	0.968	0.674	1157	0.968	0.676	1157
3	0.974	0.395	1179	0.971	0.580	1181	0.965	0.794	1190
4	0.975	0.361	1188	0.975	0.281	1182	0.968	0.681	1194
5	0.975	0.362	1194	0.975	0.356	1192	0.973	0.466	1190

With coordinated LVRT control, the PCC voltage, the stator voltage, and the rotor speed of the IG are shown in Figures 7a–7c. With a grid fault, reactive power from the PMSG injected into the PCC increases, and thus the PCC voltage and the stator voltage of the IG are improved. The rotor speed of IG accelerates more slowly. If the resultant PCC voltage is higher than the critical voltage, the IGs will successfully ride through faults with the help of PMSGs.

7. Conclusions

This paper proposes a new analytical model to calculate the minimum number of PMSGs to help LVRT of the IGs in hybrid wind farms. The lowest PCC voltage decided by the grid rule is compared with the critical PCC voltage to judge slip stability of the IGs. To avoid slip instability, power outputs at the PCC and the PMSGs are quantified. With improved var control scheme under the capacity constraint of the GSC, the minimum number of the PMSGs is determined, which is compared with the dynamic simulation results to validate the error, as well as the contributing factors.

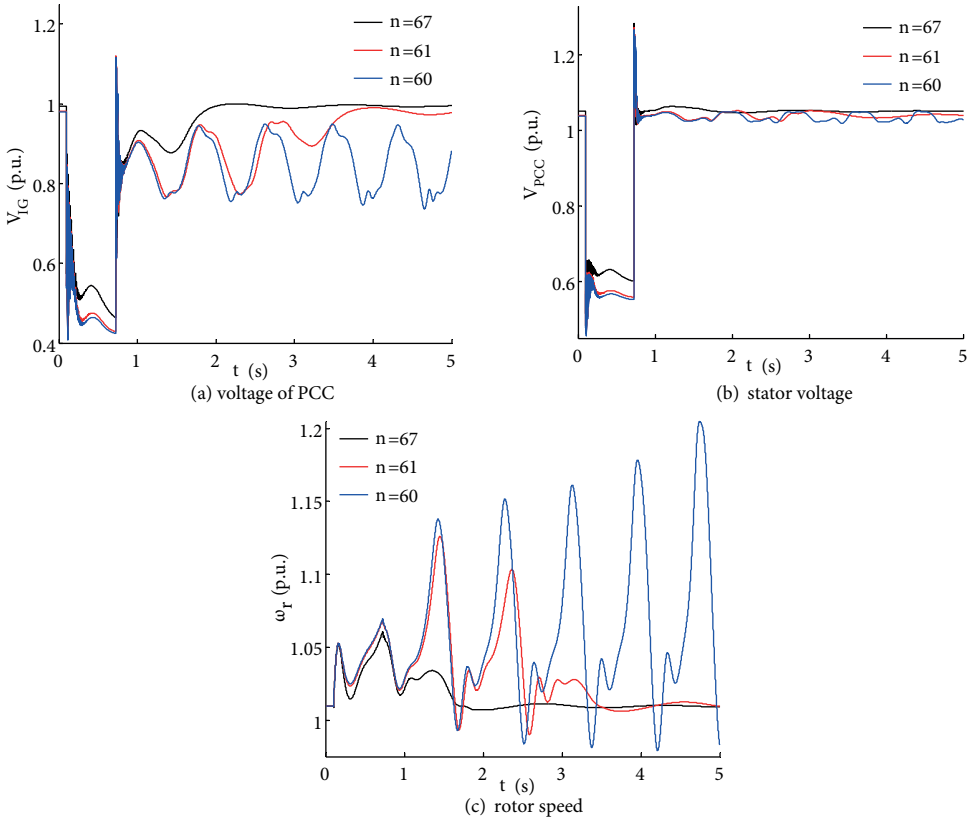

Figure 7. IG's response with coordinated LVRT.

Some conclusions are outlined as follows:

1) The critical PCC voltage for slip stability of the IG is related to the mechanical torque, the parameters of IG, and the fault duration. Larger inertia or rotor resistance of the IG, less mechanical torque or stator reactance or rotor reactance, or shorter fault duration yields lower critical voltage.

2) As to the impact on the critical PCC voltage, the mechanical torque ranks the highest, followed by the rotor reactance, the fault time, the rotor resistance, the inertia, and the stator reactance.

3) The minimum number of the PMSGs yielded by the proposed analytical model is a little more than that from dynamic simulation. The error is caused by estimation of the critical voltage as well as the average slip.

Based on the authors' experience, the critical factors for coordinated LVRT (the minimum number of PMSGs) are the voltage drop of PCC, the power capability of the WTGs, and the control strategy of the GSC. These factors are also valid for coordination with other types of WTGs if readers want to validate or extend the proposed method.

Acknowledgment

This work was supported by the National Natural Science Foundation of China (grant NSFC-51277049).

References

[1] Benchagra M, Maaroufi M, Ouassaid M. A performance comparison of linear and nolinear control of a SCIG-wind farm connecting to a distribution network. Turk J Elec Eng & Comp Sci 2014; 22: 1-11.

[2] Emanuel H, Schellschmidt M, Wachtel S, Adloff S. Power quality measurements of wind energy converters with full-scale converter according to IEC 61400-21. In: International Conference on Electrical Power Quality and Utilisation; 15–17 September 2009; Lodz, Poland. New York, NY, USA: IEEE. pp. 1-7.

[3] Amutha N, Kumar BK. Effect of modeling of induction generator based wind generating systems on determining CCT. IEEE T Power Syst 2013; 40: 4456-4464.

[4] Pedra J, Córcoles F, Monjo LI, Bogarra S, Rolán A. On fixed-speed WT generator modeling for rotor speed stability studies. IEEE T Power Syst 2012; 27: 397-406.

[5] Samuelsson O, Lindahl S. On speed stability. IEEE T Power Syst 2005; 20: 1179-1180.

[6] Mahfouz MMA, El-Sayed MAH. Static synchronous compensator sizing for enhancement of fault ride-through capability and voltage stabilization of fixed speed wind farms. IET Renew Power Gener 2014; 8: 1-9.

[7] Causebrook A, Atkinson DJ, Jack AG. Fault ride-through of large wind farms using series dynamic braking resistors. IEEE T Power Syst 2007; 22: 966-975.

[8] Abedini A, Nasiri A. Output power smoothing for wind turbine permanent magnet synchronous generator using rotor inertia. Elect Power Compon Syst 2009; 37: 1-19.

[9] Chinchilla M, Arnaltes S, Burgos JC. Control of permanent-magnet generators applied to variable-speed wind-energy systems connected to grid. IEEE T Energy Convers 2006; 21: 130-135.

[10] Kim KH, Jeung YC, Lee DC, Kim HG. LVRT scheme of PMSG wind power systems based on feedback linearization. IEEE T Power Electron 2012; 27: 2376-2384.

[11] Nguyen TH, Lee DC. Advanced fault ride-through technique for PMSG wind turbine systems using line-side converter as STATCOM. IEEE T Ind Electron 2013; 60: 2842-2850.

[12] Li S. Operation region of doubly fed induction generators based on rotor slip under maximum power point tracking control and power dispatch. Elect Power Compon Syst 2014; 42: 808-817.

[13] Li S. Power flow modeling to doubly-fed induction generators under power regulation. IEEE T Power Syst 2013; 28: 3292-3301.

[14] Molinas M, Suul JA, Undeland T. Low voltage ride through of wind farms with cage generators: STATCOM versus SVC. IEEE T Power Electron 2008; 23: 1104-1117.

[15] Teninge A, Roye D, Bacha S, Duval J. Low voltage ride-through capabilities of wind plant combining different turbine technologies. In: European Conference on Power Electronics and Applications; 8–10 September 2009; Barcelona, Spain. New York, NY, USA: IEEE. pp. 1-9.

[16] Muyeen SM, Takahashi R, Murata T, Tamura J. A variable speed wind turbine control strategy to meet wind farm grid code requirements. IEEE T Power Syst 2010; 25: 331-340.

[17] Sarkhanloo MS, Yazdankhah AS, Kazemzadeh R. A new control strategy for small wind farm with capabilities of supplying required reactive power and transient stability improvement. Renew Energ 2012; 44: 32-39.

[18] Rosyadi M, Muyeen SM, Takahashi R, Tamura J. Stabilization of fixed speed wind generator by using variable speed PM wind generator in multi-machine power system. In: IEEE International Conference on Electrical Machines and Systems; 21–24 October 2012; Sapporo, Japan. New York, NY, USA: IEEE. pp. 3292-3301.

[19] Leon AE, Mauricio JM, Gómez-Expósito A, Solsona JA. An improved control strategy for hybrid wind farms. IEEE T Sustain Energ 2010; 1: 131-141.

[20] Grilo AP, Mota ADA, Mota LTM, Freitas W. An analytical method for analysis of large-disturbance stability of induction generators. IEEE T Power Syst 2007; 22: 1861-1869.